J Mol Model (2013) 19:1937–1942
DOI 10.1007/s00894-013-1763-6

ORIGINAL PAPER

Zwitterion L-cysteine adsorbed on the Au_{20} cluster: enhancement of infrared active normal modes

Alfredo Tlahuice-Flores

Received: 10 November 2012 / Accepted: 9 January 2013 / Published online: 24 January 2013

Abstract The study reported herein addressed the structure, adsorption energy and normal modes of zwitterion L-cysteine (Z-cys) adsorbed on the Au_{20} cluster by using density functional theory (DFT). It was found that four Z-cys are bound to the Au_{20} apexes preferentially through S atoms. Regarding normal modes, after adsorption of four Z-cys molecules, a more intense infrared (IR) peak is maintained around 1,631.4 cm^{-1} corresponding with a C=O stretching mode, but its intensity is enhanced approximately six times. The enhancement in the intensity of modes between 0 to 300 cm^{-1} is around 4.5 to 5.0 times for normal modes that involve O–C=O and C-S bending modes. Other two normal modes in the range from 300 to 3,500 cm^{-1} show enhancements of 6.0 and 7.4 times. In general, four peaks show major intensities and they are related with normal modes of carboxyl and NH_3 groups of Z-cys.

Keywords Gold 20 · Normal mode · Amino acid · Zwitterion L-cysteine

Introduction

The study of small gold clusters and their striking properties due to their reduced size and shapes are the focus of intense research nowadays. The interaction between gold clusters and organic molecules constitutes an interesting topic due to its implications in biologic systems and in advancing our understanding of these novel systems in general. The Au_{20} cluster was first reported in 2003 by the group of L-S Wang [1], in a combined theoretical and photoelectron spectroscopy study determining its high stability in accordance with a high HOMO–LUMO (HL) gap of 1.77 eV, which is higher than HL gap of the C_{60} molecule. Moreover, a T_d symmetry and its bond distances were established in the range 2.16–3.12 Å [1]. In 2008, by means of vibrational spectroscopy, Fielicke's group showed that the infrared (IR) spectrum of a neutral Au_{20} cluster has a maximum at 148 cm^{-1}, which corresponds with a normal mode with a T_2 irreducible representation [2]. Regarding functionalization of the Au_{20} cluster, Zhang et al. [3] successfully synthesized in aqueous solution an Au_{20} cluster coordinate with eight triphenyl phosphine ligands, finding four ligands bound to the apexes, anticipating its catalytic applications. On the other hand, calculations performed on the Au_{20} gold cluster were reviewed in a paper by Kryachko [4]. In those previous reports, the BP86 functional was established as the best functional with which to estimate a HL gap closely related to the experimental value [5], and the Perdew-Burke-Ernzerhof (PBE) functional with a double basis set including d polarization functions (DSPP) gave the best value of the IR maximum [6]. The high stability of the Au_{20} cluster is due to both its large HL gap and its lack of fluxionality at 300 K (interconversion between minima) as determined by Born-Oppenheimer molecular dynamics simulations [7]. More recently, Palmer et al. [8, 9] obtained atomic-resolution images of the Au_{20} cluster using aberration-corrected scanning transmission electronic microscopy, confirming its T_d symmetry.

The amino acid cysteine is a simple chiral molecule (C_1 point group) built from thiol (SH), amino (NH_2) and carboxyl (COOH) functional groups. However, it is well known that amino acids in aqueous solution are in their zwitterion forms, while their neutral forms are unstable in the gas phase; previous studies have thus used dianions, monoanions and metal ions to stabilize amino acid zwitterions [8, 9].

The structure of enantiomeric L-cysteine (L-cys; 2-amino-3-thiol propane carboxyl acid) has been determined previously by

A. Tlahuice-Flores (✉)
Department of Physics and Astronomy, University of Texas at San Antonio, One UTSA Circle,
San Antonio, TX 78249, USA
e-mail: tlahuicef@gmail.com

means of an X-ray study in which an orthorhombic and monoclinic phase was present in the crystal, which exhibited the zwitterion form ($HS–CH_2–CH–NH_3^+–COO^-$) (named as Z-cys in this work) [10, 11]. Amino acids are intrinsically flexible in the gas phase, showing in their neutral form conformers that are close in energy [12, 13]. Raman and IR spectra of gas phase L-cys were reported and their frequencies assigned previously [14]. Between the normal modes of L-cys, the S–H stretching mode is relevant because it occurs in a spectral range where no other vibrations are present, and it can be used as a sensitive probe of the neighborhood. In addition, it is known that, after adsorption of L-cys on gold clusters, the S–H stretching mode disappears. In aqueous solution, the frequency of S–H stretching mode of Z-cys has been reported as 2,546 or 2,540 cm^{-1} [15].

Normal mode calculations are important in the prediction of new systems as they can be used to determine harmonic frequencies, which can then be compared with those obtained experimentally. It is well known that IR spectroscopy can detect certain chemical groups forming part of a molecule.

This report addresses the calculations of a system formed by four L-cys adsorbed onto the Au_{20} cluster in aqueous solution. Interest is focused on the preferential sites of adsorption, the binding energies and on the normal modes of the system Z-cys/Au_{20}. The aim of this study was to understand the interactions between the Au_{20} cluster and amino acids such as Z-cys and, by means of their calculated IR spectra, to determine features of these interactions. The study consisted of four stages: (1) optimization of each interacting molecule in aqueous phase, (2) determination of the more stable adsorption sites of one Z-cys on the Au_{20} cluster, (3) analysis of structure of four Z-cys molecules on the Au_{20} cluster, and (4) comparison between IR spectra before and after adsorption.

Methods

Density functional theory (DFT) calculations were carried out within the generalized gradient approximation (GGA). The Perdew-Burke-Ernzerhof (PBE) [16] functional and a DFT semi-core pseudopotentials (DSPP) treatment were employed in all calculations. This treatment of the core substitutes the effect of the core electrons by a simple potential and some degree of relativistic effects. A double numerical plus polarization (DNP) is used, taking into account that it includes a polarization p-function on all hydrogen atoms. Structural optimizations were performed without symmetry restrictions, using a force tolerance criterion of 0.002 Harthree/Å. The choice of a basis set that includes polarization functions is based on reports showing that these functions have an influence on the prediction of intensities [17, 18]. Solvation effects were considered by using the conductor-like screening model (COSMO) [19–21], which uses a scaled conductor boundary condition instead of the much more complicated dielectric boundary condition for the calculation of the polarization charges of a molecule in a continuum, being a considerable simplification of the approach developed by Tomasi and co-workers [22] without significant loss of accuracy, allowing a more efficient implementation of the continuum solvation model (CSM) and accurate calculation of gradients, which allows geometry optimization of the solute within the dielectric continuum. All methodology mentioned (PBE/DNP) is implemented in the $Dmol^3$ package [23–25]; note that this methodology reproduces both the experimental HL gap of the Au_{20} cluster and the IR spectrum of Z-cys.

Previous to the study of the Z-cys/Au_{20} system, the binding energy (E_b) of Z-cys on different Au_{20} sites was estimated using the following expression:

$$E_b = E(nZ-cys/Au_{20}) - [E(Au_{20}) + E(nZ-cys)] - nE(H_2)/2, \quad (1)$$

Where, $E(Au_{20})$ is the total energy of the pure Au_{20}, E(nZ-cys) is the total energy of n zwitterion L-cys molecules, and $E(n$Z-cys/$Au_{20})$ is the total energy of the system built by n molecules of Z-cys adsorbed on the Au_{20} cluster. $E(H_2)/2$ is the total energy of one hydrogen atom and this term takes into account that once one Z-cys is bound to the Au_{20} cluster, one H atom is released. A negative E_b value indicates that the system is viable.

It is important to note that we considered Z-cys throughout this report because the experimental data used for comparison were obtained in aqueous solution [26].

Results and discussion

Prior to the study of the Z-cys/Au_{20} system, it was carried out the structural and vibrational study of each molecule. In the following is discussed the obtained results.

The Au_{20} cluster

The Au_{20} cluster in aqueous solution considered in the COSMO model maintained its T_d symmetry as in the gas

Table 1 Twenty-three irreducible normal modes of the Au_{20} cluster optimized in aqueous phase and their irreducible representation (Γ)

Γ	Frequency, cm^{-1}
A_1	38.2, 45.8, 85.3, 98.2, 181.4
E	30.2, 44.4, 52.7, 110.0, 165.6
T_1	16.2, 54.5, 94.3, 106.6
T_2	27.2, 38.2, 44.1, 54.0, 66.5, 73.1, 116.5, 133.2, 173.5

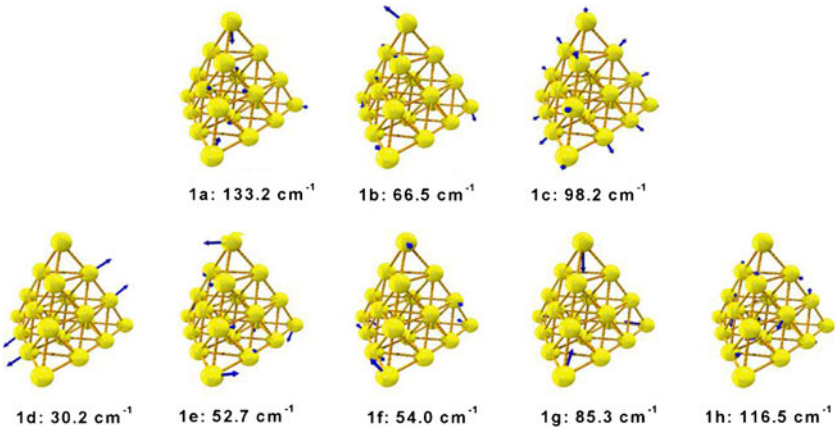

Fig. 1 **a**–**h** Selected normal modes of the Au_{20} cluster calculated using COSMO/PBE/DNP

phase. The cluster contains surface atoms bound with 54 bonds, which are distributed in the following manner: 6 bonds are located at the middle of edges (2.71 Å), 12 at the ends of edges (2.75 Å), 24 between the central Au atom on faces and their six neighbors (2.86 Å), and 12 bonds at short diagonals on faces (3.0 Å). These calculated bonds are in agreement with distances reported by Fielicke [2].

The Au_{20} cluster with a T_d symmetry has 54 normal modes with irreducible representation given as $\Gamma=5A_1+5E+4T_1+9T_2$. The A_1 and E normal modes are Raman active, T_1 are inactive both in IR and Raman, and T_2 normal modes are Raman and IR actives. Due to the known incapacity of DFT functionals to reproduce the measured maximum of IR spectra located at 148 cm^{-1}, a reportedly more accurately methodology was selected in this study [6]. The PBE/DNP methodology used yielded an HL gap of 1.9 eV, which is in agreement with the experimental value of 1.8 eV [1]. The calculated normal modes of the neutral Au_{20} cluster in aqueous phase and its irreducible representations are listed in Table 1. The IR spectrum of the Au_{20} cluster shows a maximum at 133.2 cm^{-1}, which correspond with a T_2 stretching normal mode (Fig. 1a). A threefold degeneracy bending normal mode is located at 66.5 cm^{-1} (Fig. 1b). Raman active modes are expected at 38.2, and 45.8 cm^{-1}, which are symmetric bending modes, another stretching mode is located at 85.3 cm^{-1}, while an intense breathing mode (A_1) is at 98.2 cm^{-1} (Fig. 1c). A further two peaks with a T_2 irreducible representation are located at 116.5 and 73.1 cm^{-1}. Figure 1 depicts other selected normal modes and Fig. 3a shows a stick representation of the calculated IR spectrum.

The Z-cys molecule

The literature reports three studies that used two different conformers of L-cys in zwitterion form. Those conformers were reoptimized, finding that the conformer reported by Foley and Enescu [26] is 0.11 eV more stable than that reported by Pawlukojc et al. [15] and Diaz-Fleming et al. [27]. It is important to note that the more stable Z-cys has its S–H bond oriented toward the COO^- group in a similar way to

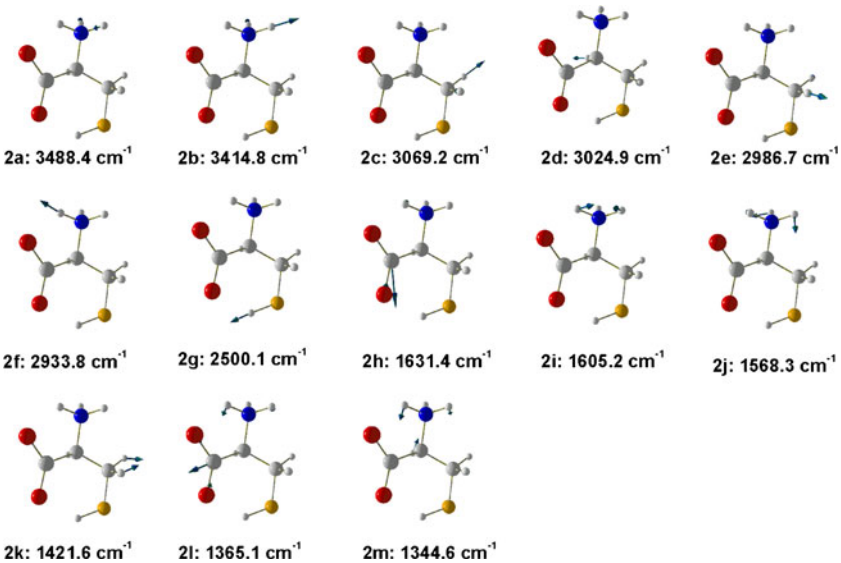

Fig. 2 **a**–**m** Selected normal modes of Z-cys calculated using COSMO/PBE/DNP

Table 2 Comparison of calculated (not scaled) frequencies of Z-cys and Z-cys/Au_{20} with experimental data

Assignment	Z-cys, cm^{-1}	Z-cys/Au_{20}, cm^{-1}	Experimental frequencies [15, 26]
NH_3^+ stretching. asymmetric	3,488.4	3,487.4	3,190
NH_3^+ stretching symmetric	3,414.8	3,408.9	3,000/3,001
C_β–H_2 stretching asymmetric	3,069.2	3,005.8	/2,959
C_β–H_2 stretching symmetric	2,986.7	3,048.4	2,970/2,837
C_α–H stretching	3,024.9	3,054.9	
N–H stretching	2,933.8	3,025.8	2,540/2,581
S–H stretching	2,500.1		
C=O stretching	1,631.4	1,628.4	
NH_2 scissors	1,605.2	1,606.6	1,611/1,647

that in the gas phase structure [12, 13]. The calculated structure of Z-cys coincides with the conformer reported by Dobrowolski et al. [28], and shows a C_1 structure with 13 bonds that are distributed as follows: two N–H bonds (1.03 Å) and one N–H bond (1.06 Å) directed toward the O atom of carboxyl; three C–H bonds (1.10 Å) including C_α and C_β atoms; one C=O bond (1.26 Å) and one C–O bond (1.27 Å) forming the COO^- group; one S–H bond (1.37 Å), a N–C bond (1.50 Å), a C_α–C_β bond (1.53 Å), one C_α–COO^- (1.57 Å), and a S–C_β bond (1.84 Å). Due to Z-cys exhibiting a C_1 symmetry its spectrum shows various peaks that correlate with its 36 normal modes with an irreducible representation A_1. The IR spectrum show peaks in the range 2,000–3,500 cm^{-1} that are correlated with the following modes: N–H_2 asymmetric and symmetric stretching modes are at 3,488.4 and 3,414.8 cm^{-1} respectively; C_β–H asymmetric and symmetric stretching modes are at 3,069.2 and 2,986.7 cm^{-1}; C_α–

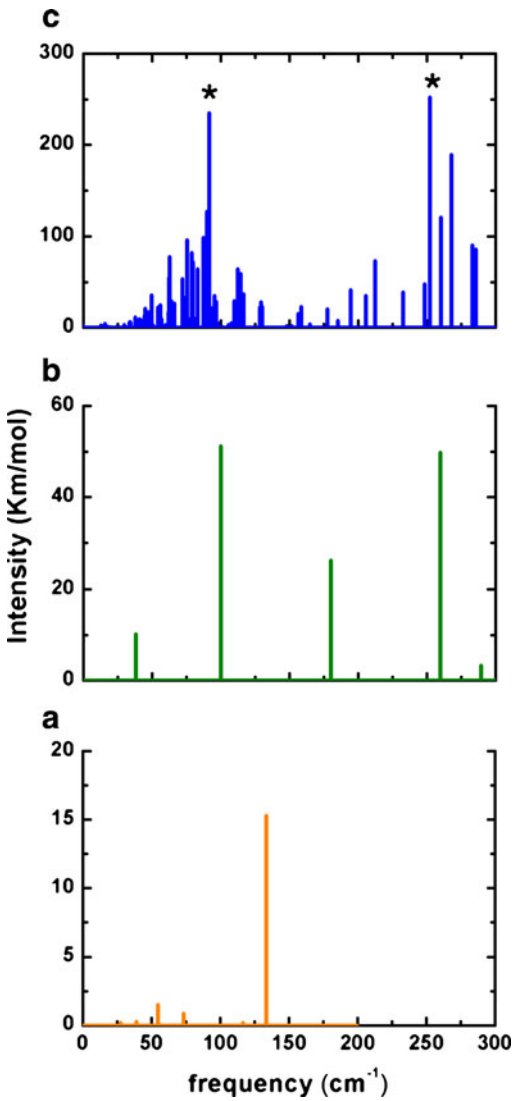

Fig. 3 Calculated infrared (IR) stick spectra of **a** Au_{20}, **b** Z-cys and **c** four Z-cys on the Au_{20} cluster in the range from 0 to 300 cm^{-1}. *Asterisks* indicate two enhanced peaks. Note the different scales used in the intensity axis

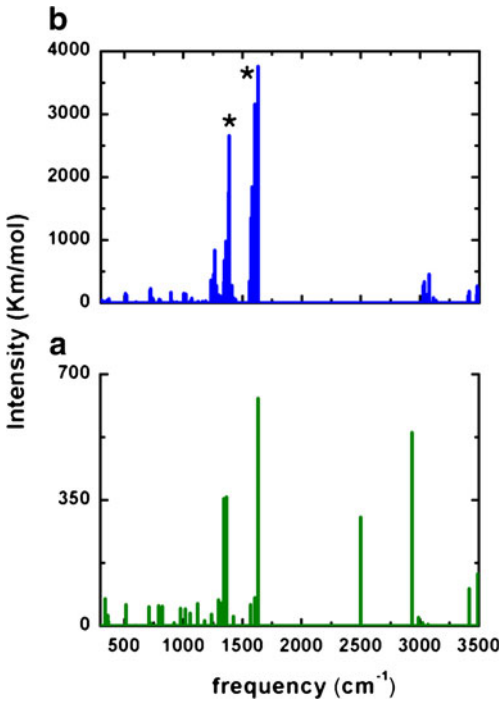

Fig. 4 Calculated IR stick spectra of **a** Z-cys and **b** four Z-cys on the Au_{20} cluster in the range from 300 to 3,500 cm^{-1}. *Asterisks* indicate two enhanced peaks. Note the different scales used in the intensity axis

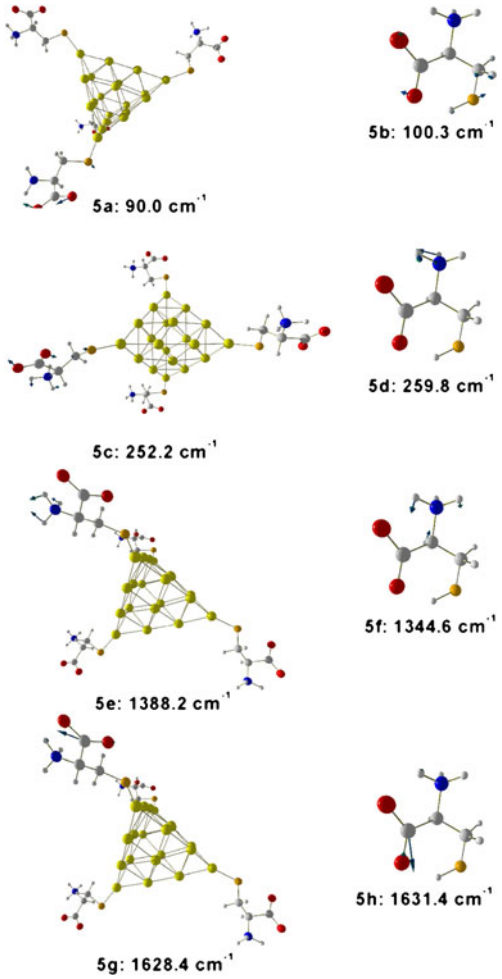

Fig. 5 Four enhanced normal modes of four Z-cys on the Au_{20} cluster and their corresponding Z-cys modes

H stretching mode is at 3,024.9 cm^{-1}; the N–H mode is located at 2,933.8 cm^{-1}; and the S–H stretching mode is located at 2,500.1 cm^{-1}. The more intense peak is located at 1,631.4 cm^{-1} (Fig. 2h) and corresponds with a C=O stretching mode. Two NH_2 scissors modes are located at 1,605.2 and 1,568.3 cm^{-1}. A C_β–H_2 scissor mode is present at 1,421.6 cm^{-1}. The NH_3 umbrella bending mode is located at 1,344.6 cm^{-1}. Figure 2 shows the modes mentioned, their assignment; their comparison with experimental data is listed in Table 2. The calculated IR spectra of the Z-cys molecule can be seen in Figs. 3b and 4a.

The Z-cys/Au_{20} system

In order to verify the accuracy of methodology used, the binding energy of the Au_{20}-formyloxyl system was estimated, finding a value of 1.8 eV, which is in agreement with the reported value of 1.76 eV [29]. After considering systematically different binding sites on the Au_{20} cluster, and conformations of the adsorbed Z-cys, it is concluded that one Z-cys prefers to bind to the apexes of the Au_{20} cluster through the S atom. Adsorption of one Z-cys through the S atom on the Au_{20} face is 0.51 eV energetically less viable with respect to one Z-cys (calculated low adsorption energy) adsorbed on an apex of the Au_{20} cluster. It was found that one Z-cys adsorbed to the Au_{20} cluster shows a low adsorption energy and, after four Z-cys molecules bind to the Au_{20} cluster apexes, the binding energy increases to 0.13 eV.

The optimized Au_{20} with four Z-cys in aqueous solution shows 106 bonds, with S–Au bonds having an average length of 2.33 Å, and three types of Au–Au bonds close to one apex (2.78, 2.77 and 2.81 Å) while these bonds in the Au_{20} cluster were 2.75 Å. In general, the bond distances of Z-cys adsorbed on Au_{20} varied slightly after adsorption. The C=O bonds were 1.27, and C–O bonds 1.26 Å. The eight N–H bonds (1.03 Å) and four N–H bond (1.05 Å) directed toward the O atom of carboxyl are similar to the bond distances found on Z-cys.

The IR spectrum of four Z-cys adsorbed on the Au_{20} cluster can be split in two regions: the range 0–300 cm^{-1} (Fig. 3c) where the Au_{20} cluster and Z-cys normal modes occurs, and 300–3,500 cm^{-1} (Fig. 4b) where Z-cys normal modes are present. Five IR peaks of Z-cys are located in the 0–300 cm^{-1} region, the largest of which presents an intensity of 51.21 km mol^{-1}, while, in the case of the Au_{20} cluster its maximum located at 133.2 cm^{-1} shows an intensity of 15.31 km mol^{-1}. Two peaks are present in the Z-cys/Au_{20} system, with enhanced intensity of around 4.6- and 5-times for peaks located at 90.0 (Fig. 5a) and 252.2 cm^{-1} (Fig. 5c), which can be related to peaks at 100.3 and 259.8 cm^{-1} on free Z-cys, respectively. The peak located at 100.3 cm^{-1} corresponds to a coupled O–C=O rocking with a C–S bending mode. The peak located at 252.2 cm^{-1} shows the NH_3 torsion movement of the 259.8 cm^{-1} peak on Z-cys but also involving S, O, and C atoms.

Two intense peaks located at 1,388.2 (NH_3 umbrella bending) and 1,628.4 cm^{-1} (C=O stretching) are observed in the region from 300 to 3,500 cm^{-1} of Fig. 4b, which correspond with 1,344.6 and 1,631.4 cm^{-1} (Fig. 5h) on the Z-cys molecule. The 1,388.2 cm^{-1} peak is enhanced 7.4-times while the 1,628.4 cm^{-1} peak is 6-times more intense. It is important to note that the peak due to NH_3 umbrella bending is the more affected in its position after adsorption of Z-cys, the difference being around 44 cm^{-1}. Figure 5 depicts the four enhanced IR active normal modes mentioned above, and Table 2 reports the calculated frequencies and comparison with experimental data.

Conclusions

Here, we report on a study of the zwitterion L-cys adsorbed onto the Au_{20} cluster. The study of separate Au_{20} and Z-cys molecules prior to their interaction reproduced previously reported experimental data (HL gap and IR spectrum). A low

adsorption energy of the four Z-cys on the Au_{20} cluster was determined. Based on calculated IR spectra, it was concluded that the main effect is the enhancement of the intensities of four IR peaks located at 90.0, 252.2, 1,388.2 and 1,628.4 cm^{-1} that involve carboxyl and NH_3 groups. The position and the number of the enhanced peaks can be varied by using other gold clusters that exhibit a higher adsorption energy of Z-cys molecules. In the case of the Au_{20} cluster, the enhanced IR normal modes do not involve gold atoms. Further experimental studies will be necessary to confirm the obtained enhancement of the four IR peaks.

Acknowledgments The author acknowledges the Consejo Nacional de Ciencia y Tecnología, the Departamento de Supercómputo of Universidad Nacional Autónoma de México, and the National Science Fundation (NSF) for support with grants DMR-1103730, "Alloys at the nanoscale: the case of nanoparticles second phase and PREM: NSF PREM Grant # DMR 0934218; "Oxide and metal nanoparticles—the interface between life sciences and physical sciences"

References

1. Li J, Li X, Zhai HJ, Wang LS (2003) Science 299:864–867
2. Gruene P, Rayner DM, Redlich B, van der Meer AFG, Lyon JT, Meijer G, Fielicke A (2008) Science 321:674–676
3. Zhang HF, Stender M, Zhang R, Wang C, Li J, Wang LS (2004) J Phys Chem B 108:12259–12263
4. Kryachko ES, Remacle F (2007) Int J Quantum Chem 107:2922–2934
5. Molina B, Soto JR, Calles A (2008) Rev Mex Fis 54:314–318
6. Yang A, Fa W, Dong J (2010) Phys Lett A 374:4506–4511
7. Vargas A, Santarossa G, Iannuzzi M, Baiker A (2009) Phys Rev B 80:195421-1–195421-13
8. Wang ZW, Palmer RE (2012) Nanoscale 4:4947–4949
9. Yang G, Zu Y, Liu C, Fu Y, Zhou L (2008) J Phys Chem B 112 (23):7104–7110
10. Görbitz HC, Dalhus B (1996) Acta Cryst C 52:1756–1759
11. Moggach SA, Clark SJ, Parson S (2005) Acta Cryst E 61:o2739–o2742
12. Wilke JJ, Lind MC, Schaefer HF III, Császár AG, Allen WD (2009) J Chem Theor Comput 5:1511–1523
13. Roux MV, Foces-Foces C, Notario R, Ribeiro da Silva MAV, Ribeiro da Silva M, das Dores MC, Filipa A, Santos LOM, Juaristi EJ (2010) Phys Chem B 114:10530–10540
14. Gargaro AR, Barron LD, Hecht LJ (1993) Raman Spectrosc 24:91–96
15. Pawlukojc A, Leciejewicz J, Ramirez-Cuesta AJ, Nowicka-Scheibe J (2005) J Spectrochim Acta A 61:2474–2481
16. Perdew JP, Burke K, Ernzerhof M (1996) Phys Rev Lett 77:3865–3868
17. Bernhard HS (1999) J Chem Phys 111:8819–8824
18. Jiménez-Hoyos CA, Janesko BG, Scuseria GE (2008) Phys Chem Chem Phys 10:6621–6629
19. Klamt A, Schüürmann GJ (1993) Chem Soc Perkin Trans 2:799
20. Klamt A, Jonas V, Burger T, Lohrenz J (1998) J Phys Chem 102:5074
21. Delley B (2006) Mol Simul 32:117–123
22. Cossi M, Barone V, Cammi R, Tomasi J (1996) Chem Phys Lett 255:327–335
23. Delley B (2002) Phys Rev B 66:155125
24. Delley B (1990) J Chem Phys 92:508
25. Delley B (2000) J Chem Phys 113:7756
26. Foley S, Enescu M (2007) Vib Spectrosc 44:256–265
27. Diaz Fleming G, Finnerty JJ, Campos-Vallette M, Célis F, Aliaga AE, Fredes C, Koch Rainer J (2009) Raman Spectrosc 40:632–638
28. Dobrowolski JC, Rode JE, Sadlej J (2007) THEOCHEM 810:129–134
29. Hull JM, Provorse MR, Aikens CM (2012) J Phys Chem A 116:5445–5452